THE ASTROPHYSICAL JOURNAL, 414:316–332, 1993 September 1

CNO ABUNDANCES AND THE EVOLUTIONARY STATUS OF THREE A-TYPE SUPERGIANTS

KIM A. VENN
Department of Astronomy, University of Texas at Austin, RLM 15.308, Austin, TX 78712
Received 1992 November 5; accepted 1993 March 5

ABSTRACT

Abundance results are presented for three massive ($\sim 10\ M_{\odot}$), Population I A-type supergiants; HD 13476 (A3 Iab), HD 46300 (A0 Ib), and HD 87737 (A0 Ib). Equivalent widths of weak CNO and metal lines have been collected from high signal-to-noise CCD spectra. Atmospheric parameters ($T_{\rm eff}$ and gravity) are determined from spectroscopic indicators since Strömgren colors are not well calibrated for these stars. Observed Hγ profiles are compared to those generated from Kurucz's line-blanketed model atmospheres, and ionization equilibrium of Mg I/Mg II is used to choose the final model parameters. Ionization equilibrium of Fe I/Fe II is also calculated but not used explicitly since large non-LTE effects are predicted for Fe I lines.

We find these A supergiants have roughly solar metal abundances (i.e., [M/H] = +0.1 to −0.3 for Fe, Mg, Ti, and Cr). There are large enrichments of nitrogen ([N/H] ~ +0.8), accompanied by slight carbon and possibly oxygen depletions. These are consistent with the predictions for CNO-processed envelopes of post-red supergiant stars that have undergone the first dredge-up mixing event. In support of this, the sum [(C+N+O)/Fe] = 0.0 to 0.1 for all three stars and the nitrogen enhancement appears correlated with the carbon and oxygen deficits as expected for CNO-cycled gas. However, the ratios [N/C] and [N/O] are larger than most first dredge-up predictions by 0.3–0.6 dex. This may indicate additional mixing of CNO-cycled gas, significant mixing of ON-cycled gas to drive up the nitrogen abundances, or that CNO-cycling alone is not responsible for the abundance pattern. Thus, the nitrogen enhancements indicate a complex chemical evolutionary history for these stars, or a systematic error in the classical analysis of N I lines in A supergiant atmospheres, for example, large non-LTE corrections.

Subject headings: stars: abundances — stars: evolution — stars: interiors — supergiants

1. INTRODUCTION

Stellar evolution calculations predict the massive ($\sim 10\ M_{\odot}$), Galactic A supergiants are in a phase of helium-core burning. In most calculations, helium ignition occurs during a previous red supergiant phase; however, an alternative scenario is that the A supergiants have evolved directly from the main sequence. The differences between these scenarios depend on the input assumptions (e.g., convection criterion, semiconvection, convective overshoot of the core, and mass-loss rates). A review of the predictions of evolution calculations as they depend on the input physics for massive stars (about 10–30 $M_{\odot}$) is given by Fitzpatrick & Garmany (1991). If a massive star evolves quickly off the main sequence to the red giant branch (RGB), then the development of a deep surface convection zone mixes gas from hydrogen-burning layers to the outer observable layers. This process is known as the first dredge-up. Hydrogen burning on the main sequence primarily occurs via the CNO-cycle in these stars, thus the surface abundances of carbon, nitrogen, and oxygen will be altered (C slightly decreased, N enriched, and O not significantly affected) with the sum of the nuclei remaining constant since they only act as catalysts in the tri-cycle. After helium-core burning is initiated on the RGB, the star moves back to the blue region of the Hertzsprung-Russell diagram where it remains in thermal equilibrium as an A supergiant until the end of core-helium burning. In this scenario, the path of the evolutionary track on the HR diagram describes a "blue-loop." Predictions of how far back into the blue (to higher effective temperatures) the star evolves also depend on the input assumptions.

The CNO abundances in normal, Galactic A supergiants have not been previously examined. These abundances may be important in testing evolution predictions and constraining the input assumptions, particularly the treatment of convection. In this paper we present CNO abundance results for three supergiants: HD 87737 (=η Leo, A0 Ib), HD 46300 (=13 Mon, member of Mon OB1, A0 Ib), and HD 13476 (member of Per OB1, A3 Iab). General properties of these stars are presented in Table 1, including UBV and $uvby\beta$ photometric colors, Galactic location, radial velocity, and rotational velocity. We wish to establish CNO abundances in normal A supergiants, and to compare the results to CNO abundances in B-type and F-K supergiants to study massive star evolution across the upper HR diagram. These abundances may also be used as comparisons for the more unusual A-type supergiants (such as the Population II, the high Galactic latitude, and the alleged anomalous A supergiants discussed below). The stars presented here are MK standards and most likley single stars, with the possible exception of HD 87737. Hill, Walker, & Yang (1986) report this star is an eclipsing binary, and Blazit et al. (1977) made a detection of a companion at a separation of 0".039 from speckle interferometry. Photometric variability has been studied in HD 13476; this star is microvariable, where $\Delta(B-V) \sim 0.04$ mag with about a 15 day period (Percy & Welch 1983). HD 46300 is not known to be variable (van Genderen 1989). Studies on microvariability by Rosendhal (1970) found that noticeable equivalent width changes occur only in the strongest lines ($W_{\lambda} > 100$ mÅ), and Hutchings (1976) determined that changes in the Hγ line profiles are very small (<10%). We do not consider microvariability a significant problem in this weak line analysis.

1.1. *Previous Abundance Analyses of A Supergiants*

Galactic A supergiants have near solar metal abundances as determined by several authors (Lobel et al. 1992; Aydin 1972;

TABLE 1

CHARACTERISTICS OF PROGRAM STARS

HD	13476	87737	46300
spec.type	A3 Iab	A0 Ib	A0 Ib
gal.long, l (°)	133	220	204
gal.lat, b (°)	−3	+51	−1
rad.vel,(km s^{-1})[a]	−41	+3	+12
v*sini*, (km s^{-1})[a]	≤ 45	20	17
Photometric colors:[b]			
V	6.43	3.52	4.50
(B-V)	+0.60	−0.03	0.00
(U-B)	+0.24	−0.16	−0.17
(b-y)	0.477	0.030	0.050
m_1	−0.065	0.068	0.064
c_1	1.202	0.966	0.989
β	2.635	2.651	2.647
reddening:[c]			
$(B-V)_0$	0.06	0.00	0.00
E(B-V)	+0.54	−0.03	0.00
E(b-y)	0.377	−0.022	0.000

[a] From the Bright Star Catalog.

[b] Photometric indices are from the SIMBAD data base.

[c] Intrinsic $(B-V)_0$ values are based on spectral type calibrations from Fitzgerald 1970. Interstellar reddening $A_v = 3.0E(B-V) = 4.3E(b-y)$ from Crawford 1974.

Wolf 1971; Przybylski 1969; Groth 1961). The only two CNO analyses for Population I A supergiants known to us are for the A0 Ib star η Leo (HD 87737) by Lambert, Hinkle, & Luck (1989) and for the B9 Iab star σ Cyg (HD 202850) by Ivanova & Lyubimkov (1990). The latter analysis finds σ Cyg to have near solar metal abundances with an overabundance of helium and nitrogen, and a carbon deficiency; thus they conclude that the supergiant has passed through the phase of deep mixing. The study by Lambert et al. (1989) of HD 87737 also finds near solar metal abundances and CNO abundances that indicate deep mixing. However, the carbon abundance for HD 87737 is based on upper-limit equivalent width values only, and Lambert et al. do not discount non-LTE effects as the cause of the large nitrogen abundance. Also, a solar boron abundance is reported for HD 87737 by Boesgaard & Heacox (1978) from a low signal-to-noise Copernicus satellite spectrum of the B II line at λ1362. If boron is not depleted in the atmosphere of this star, then it implies that there has been little mixing with the deeper, hotter stellar layers (which would destroy boron). This would contradict first dredge-up abundances for CNO.

The chemical compositions of the high Galactic latitude A-F supergiants are quite different from normal Population I abundances. The recent examination of these stars by Luck, Bond, & Lambert (1990) determines that they are slightly metal poor ([Fe/H] = −0.35), and the CNO elements are each overabundant. HD 87737 has a high Galactic latitude (+51°), but it does not share the characteristics of the high Galactic latitude supergiants discussed by Luck et al., such as the low iron abundance; it is most likely a normal, massive star oddly located high above the Galactic plane. Normal Population I A supergiants are also easily distinguished from the metal-poor Population II A supergiants. For example, the iron abundance of HD 46703 has been determined as 1.6 dex below solar by Luck & Bond (1984), although Bond & Luck (1987) suggest the atmosphere of this A supergiant may be hydrogen deficient and predict the original iron abundances may have been as much as 2.5 dex less than solar.

Also we note that a group of alleged anomalous A supergiants have been reported in the Magellanic Clouds by Humphreys, Kudritzki, & Groth (1991). These stars are reported to have hydrogen line strengths and discontinuities that are too strong for their high luminosities, and therefore anomalous *UBV* colors. They propose that this effect is the result of an extreme helium enrichment in the stellar atmosphere (helium could comprise 30%–50% of the atmosphere). Indeed, the theoretical predictions for an increase in the helium abundance can reproduce the reported anomalies, but the requisite high helium abundances have not been established independently from other model atmosphere parameters. Also, it has been suggested that these are normal stars which have been systematically misclassified, due to the metallicity difference between the Magellanic Clouds and the Galaxy (E. L. Fitzpatrick 1993, private communication).

1.2. *Previous CNO Analyses of Related Stars*

The slightly cooler F-G supergiants near 10 $M_\odot$ were first shown to have large N/C ratios by Parsons (1967), while most other elements were found to have abundances close to the solar values. More recently Luck & Lambert (1981, 1985) have determined CNO abundances in a large sample of Galactic F-K supergiants. They found that the surface abundances generally agree with the first dredge-up predictions by Becker & Iben (1979), supporting the post-RGB evolution scenario for stars near 10 $M_\odot$. However, Luck & Lambert also noted that the [N/C] ratios are slightly larger than predicted, and suggested that perhaps additional CN-mixing occurs in these stars, possibly due to more extensive dredge-up. They also proposed that excess mixing may occur due to meridional circulation when the stars are near the main sequence and likely to be rapidly rotating, or due to convective overshoot of the core. Significant ON-cycling to drive up the nitrogen abundances was dismissed primarily because the nitrogen excess is not well correlated with the sum of the carbon and oxygen deficits; oxygen is more resistant to CNO-processing, and it requires deeper mixing and higher temperatures to drive the ON-cycle. The abundance results by Gies & Lambert (1992) for the B-supergiants make the first two mixing mechanisms plausible. They determined that the CNO abundances appear to have been partially mixed with CN-cycled elements in some stars, and suggest that partial mixing may occur near the main sequence. This had not been predicted by stellar evolution models. Extensive mass loss is another mechanism by which the surface CNO abundances may differ from the first dredge-up predictions.

2. OBSERVATIONS AND REDUCTIONS

Equivalent widths of mostly weak C I, N I, and O I lines have been collected for the A supergiants using the 2.7 and 2.1 m telescopes at the McDonald Observatory equipped with CCD cameras at the coudé focus. Representative spectra for the CNO lines in HD 46300 are shown in Figure 1. The weak C I lines near λ7115 detected only in the cooler A3 Iab star are shown in Figure 2. The Hγ Balmer line profiles have also been observed in each star, plus weak lines of Mg I and Mg II to be used in the determination of the atmospheric parameters. A

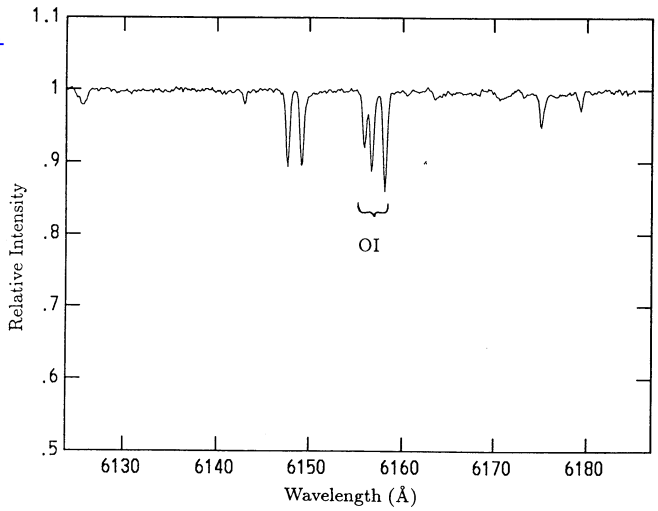

FIG. 1*a*

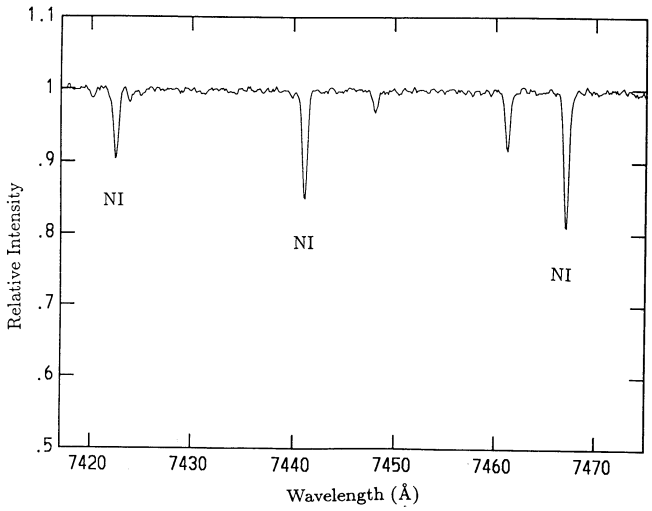

FIG. 1*b*

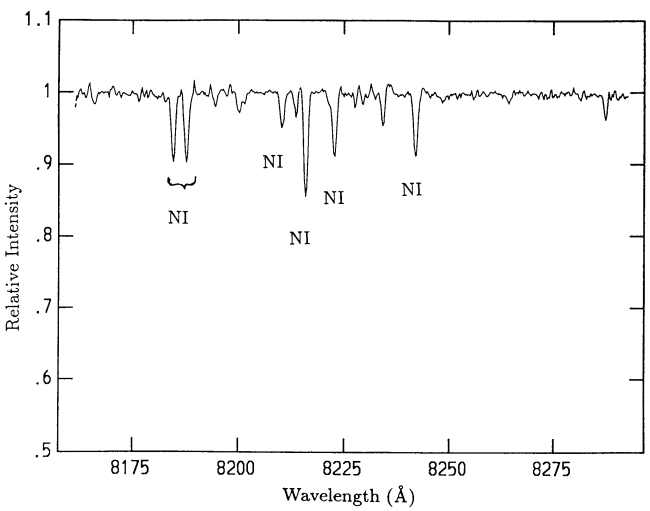

FIG. 1*c*

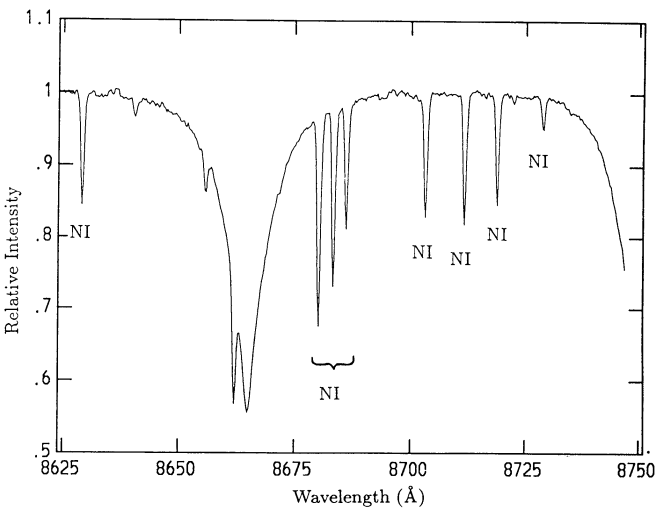

FIG. 1*d*

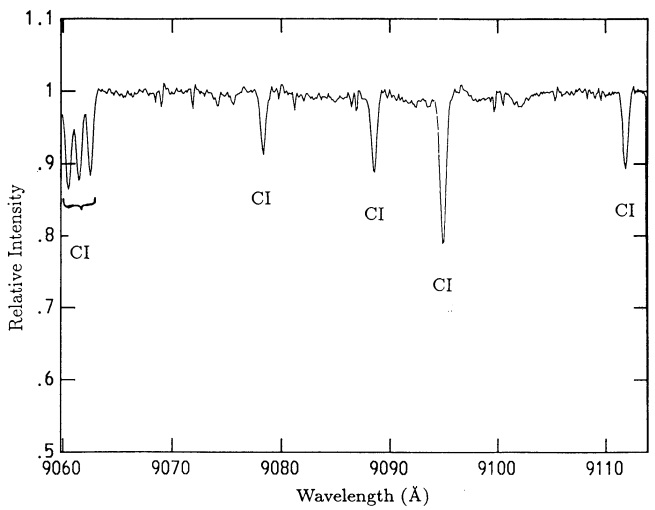

FIG. 1*e*

FIG. 1.—Spectra of O I λ6158, N I λ7440, N I λ8200, N Iλ8700, and C I λ9100 in HD 46300, respectively. The spectra at λ8200 and λ9100 have been divided by that of a rapidly rotating, hotter star to remove telluric features.

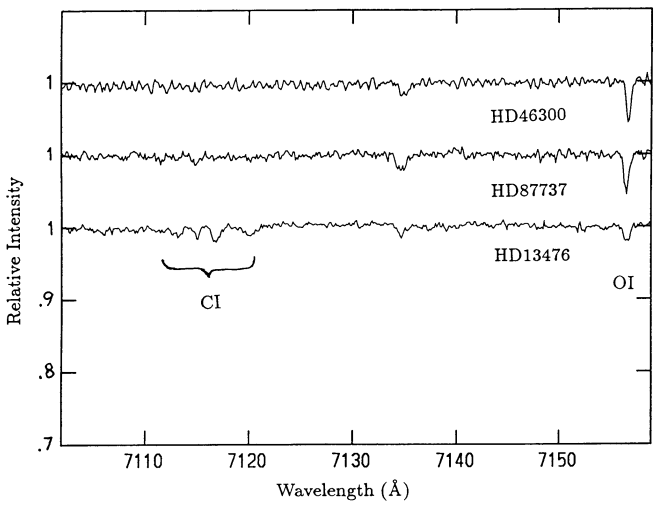

FIG. 2.—Spectra of C I λ7115 in HD 46300, HD 87737, and HD 13476; the former two are displaced for clarity. These spectra have been divided by that of a hotter, rapidly rotating star to remove the telluric features.

total of 10 (HD 87737) to 21 (HD 13476) wavelength regions have been observed, which span ~60–120 Å each. The spectra have high signal-to-noise (~80–150) and high resolution (0.07–0.25 Å pixel^{-1} depending on the grating setup).

The CCD spectra were reduced using standard IRAF[1] packages. Averaged bias frames and medianed dark frames were subtracted from the spectrum and flat lamp exposures. An averaged lamp would then be normalized and divided into spectrum frames to remove pixel-to-pixel variations across the CCD chip. Lamp frames were usually exposed to the same intensity as the spectra to avoid any nonlinearity effects in the response of the CCD detectors, although the detectors have an essentially linear response. At this stage, cosmic-ray strikes were removed if necessary. A trace of the spectrum image on the CCD was made, and several rows of pixels were co-added to obtain a one-dimensional stellar spectrum. The stellar spectrum was then rectified by fitting a smoothly varying function (such as a low-order Legendre polynomial) to the continuum; dividing by this function produced a flat spectrum where the continuum was normalized to 1. Telluric features were removed if necessary by dividing the spectrum by that of a rapidly rotating hotter star (O9-B3 stars, with $v \sin i$ greater than 120 km s^{-1}) observed near the same airmass and reduced by the same methods. Most stellar features observed in A stars are not present at much higher temperatures, and the rapid rotation guarantees that any weak lines present will be highly broadened and close to the continuum level. Telluric features were removed from the C I spectra taken near 7115 and 9100 Å, the Mg II spectra near 7880 Å, and the N I spectra near 8200 Å. After telluric features were removed, the resultant spectrum often suffered a small degradation in the signal-to-noise due to imperfect cancellation; for example, see Figures 1*c* and 1*e*. However, the continuum around the features of interest was fairly flat, which implies there were no significant spectral lines in the hot stars that were used as telluric flats; if lines were present, they would cause broad positive "bumps" in the divided continuum. In the final step, a wavelength scale was imposed on each spectrum from exposures of a hollow cathode light source (Fe, FeNe, or ThAr) taken several times throughout the observing night.

Spectral lines in each wavelength region have been identified using the Moore (1972) *Revised Multiplet Table*, except for the lines of the C I multiplet at 7115 Å (multiplets 25.02 and 26) which have been identified using the Moore (1970) C I multiplet table.

Equivalent widths (W_λ) have been measured two ways using the *splot* package in IRAF: (1) by fitting a Gaussian profile to the absorption line, and (2) by measuring the total area of the line. These W_λ values usually agreed to within 10%, which is a small uncertainty for the abundance analysis. Uncertainties in the equivalent width measurements can also arise due to the placement of the continuum level; we used the rectified continuum (at 1.0) throughout, although slight variations from this typically result in only small W_λ uncertainties (< 10%).

3. ANALYSIS

3.1. *Input Data and Assumptions*

Chemical abundances are derived from a model atmosphere analysis. Model atmospheres generated by ATLAS9 (Kurucz 1979; 1991, private communication) have been adopted which assume plane-parallel geometry, and hydrostatic and local thermodynamic equilibrium. Continuous opacity sources relevant at high temperatures (such as electron scattering) and opacities from an extensive list of metal lines are included in the opacity distribution functions. Hydrogen line opacities are also included. These assumptions are usually adequate for an analysis of photospheric lines, although A supergiants are adjacent to the regime where departures from LTE may be significant (discussed in § 3.4). A supergiant atmospheres also have very low gravities that are near the radiation pressure limit, thus it is difficult to converge the lowest gravity models in hydrostatic equilibrium, for example, for the Ia-type supergiants. This is less of a problem for the Ib-type supergiants.

The detailed analysis code WIDTH, a derivative of the ATLAS6 code, has been used to determine abundances from single spectral lines. WIDTH computes single-line elemental abundances given an input equivalent width, atomic line data, and model atmosphere generated by ATLAS9. Assuming LTE, the populations of the atomic levels in the line-forming regions are calculated, and hence the continuous line opacities. From this, a line profile is generated and theoretical equivalent width determined. By changing the abundance in this calculation, the computed width can be matched to the observed width. This code is well suited for an analysis of the A stars because it includes relevant opacity sources and broadening coefficients at high temperatures. Of course, a complete analysis for A supergiants should also include departures from LTE.

Atomic data have been gathered from a variety of sources. All atomic energy levels have been taken from Moore (1952). Oscillator strengths for Ti II, Sc II, and Fe II are from the critical compilations by Fuhr, Martin, & Wiese (1988) and Martin, Fuhr, & Wiese (1988). These authors have studied and evaluated the literature on oscillator strengths, and each value in their tables is given an estimated uncertainty. They estimate the accuracy of the lines used here as within 30%–50% (~0.15–0.25 dex). Values for a few Fe II lines not included in this compilation are taken from Fuhr et al. (1981), which is an earlier catalog of *gf*-values. Remaining Fe II lines for which

[1] IRAF is distributed by the National Optical Astronomy Observatories which is operated by the Association of Universities for Research in Astronomy, Inc., under cooperative agreement with the National Science Foundation.

gf-values could not be found from these lists or other critical evaluations were taken from the new Kurucz (1990) semiempirical calculations. This source has also provided the oscillator strengths for the Mg II lines. The Mg I *gf*-values are from the Wiese & Martin (1980) catalog of the best theoretical and experimental *gf*-values in the literature and are estimated as accurate to within 10%–25% (~0.05–0.10 dex). The Ca II values are from the critical compilation by Wiese, Smith & Miles (1969) and are estimated as accurate to within ~30% (~0.15 dex).

Fe I *gf*-values are primarily from the experimental radiative lifetime measurements and interpolation techniques of O'Brian et al. (1991). In comparing their derived oscillator strengths to other sources, they have found no significant differences from the Oxford group values (Blackwell, Petford, & Simmons 1982). They also report reasonable agreement with the Fuhr et al. (1988) compilation of the best *gf*-values in the literature within the cited uncertainties.

The Cr II values are from Sigut & Landstreet (1990) who determine astrophysical values from optical spectral lines of Vega and ι CrB. They compare their results with laboratory measurements and theoretical calculations finding excellent agreement when all values are put on an absolute scale (which has been determined based on astrophysical oscillator strengths derived from solar lines). From their derived chromium abundances, they estimate an internal scatter of less than 0.1 dex in their *gf*-values, and an uncertainty of no more than 0.15 dex in the absolute calibration.

Theoretical *gf*-values have been chosen for the O I spectral lines from Opacity Project CIV3 calculations (Hibbert et al. 1991a). These results are in excellent agreement with the astrophysically determined values by Lambert, Roby, & Bell (1982) for the λ6158 multiplet lines in the Sun. The Wiese & Martin (1980) compilation of the best *gf*-values in the literature has provided a value for a single remaining O I value (estimated accuracy is within 10%, or $\pm$0.05 dex).

Theoretical C I oscillator strengths have been adopted from Opacity Project CIV3 calculations (Hibbert et al. 1992). These values are in excellent agreement with the values calculated by Nussbaumer & Storey (1984) for multiplet 3 near λ9100, which Grevesse et al. (1991) discuss as in good agreement with recent radiative lifetime measurements. The theoretical values are also in good agreement with the solar *gf*-values calculated by Lambert et al. (1982) around λ7115. Lambert et al. (1982) adopted a solar carbon abundance that is 0.07 dex larger than assumed here, thus we adjusted the *gf*-values upwards by this amount when comparing to the Opacity Project values.

N I oscillator strengths have been collected from the experimental radiative lifetime measurements by Zhu et al. (1989). Grevesse et al. (1990) discuss sources for N I oscillator strengths and remark on the excellent agreement between the Zhu et al. values and theoretical predictions by Hibbert et al. (1991b) for the spectral lines observed in this analysis. Zhu et al. estimate the accuracy of their *gf*-values as within 15% (~ $\pm$0.05 dex).

3.2. *Atmospheric Parameters*

Photometric colors have been used for initial estimates of the atmospheric parameters (effective temperature and gravity), and then spectroscopic indicators provide the final values of $T_{\rm eff}$, gravity, and microturbulence.

UBV and *uvbyβ* indices have been obtained from the literature (see Table 1, references in the SIMBAD data base). Strömgren colors can be useful for atmospheric parameter determinations in A-F stars, although it is difficult to estimate reddening from these indices. However, the *UBV* colors can be used to estimate interstellar extinction by using the calibration by Fitzgerald (1970) of the intrinsic $(B-V)_0$ values for a given spectral type. The reddening of the Strömgren colors can then be estimated by $A_V = 3.0E(B-V) = 4.3E(b-y)$ as suggested by Crawford (1974).

Strömgren indices have been calibrated to a $T_{\rm eff}$-gravity scale for A stars by several authors using ATLAS6 model atmospheres (Lester, Gray, & Kurucz 1986; Moon & Dworetsky 1985; Relyea & Kurucz 1978). Unfortunately, the colors of the A supergiants lie outside or just at the edges of these calibrations, and often it is necessary to extrapolate. For this reason, the photometric data are employed only to make preliminary estimates. Internal uncertainties within the calibrations and reddening approximations are estimated at $\pm$200 K in $T_{\rm eff}$ and $\pm$0.2 in log g, although there appears to be larger external uncertainties between the various calibrations (as shown in Table 2). Recently Gray (1992) has derived a semiempirical effective temperature calibration for the A-F supergiants from the Strömgren colors. The temperatures calculated for the three stars in this paper are included in Table 2. Gray's calibration for the early A supergiants depends on only two stars and is therefore still somewhat uncertain.

Spectroscopic estimates of the atmospheric parameters begin with a comparison of the observed Hγ profiles with those generated from BALMER, another derivative program of ATLAS6 (see Fig. 3 for sample fits of Hγ in HD 46300). BALMER incorporates a detailed Stark broadening theory (Vidal, Cooper, & Smith 1973) such that the wings of the Balmer lines can be used reliably to determine atmospheric parameters (ignoring non-LTE effects which are discussed in § 3.4). The Balmer line cores are not reliably reproduced by the code due to neglected non-LTE effects, rotational and instrumental broadening, and possibly slight mass loss or variability. In A-type stars, the Balmer line wings depend on both temperature and gravity such that several temperature-gravity parameters may fit an observed profile. Within the range of parameters found from photometry, the locus of best Hγ line fits has been determined for each star and is shown in Figure 4. Another locus of temperature-gravity parameters can be determined from the ionization equilibrium of neutral and ionized magnesium. Ionization equilibrium demands that abundances derived from two different ionic states of an atom be the same, that is, log ϵ(Mg I) = log ϵ(Mg II). The locus of atmospheric parameters that reproduce the same magnesium abundance from both the Mg I and Mg II lines has been determined for each star and is also shown in Figure 4.

The final atmospheric parameters are chosen where the Hγ locus and Mg ionization equilibrium locus intersect on the temperature-gravity plane. The A supergiants also have spectral lines of both Fe I and Fe II which can be used in an ionization equilibrium calculation, however, non-LTE effects (discussed in § 3.4) are predicted to be quite large for Fe I lines which makes this species unreliable for the equilibrium calculations. The locus of atmospheric parameters that reproduce the same iron abundance from Fe I and Fe II is shown in Figure 4, but not used when choosing the atmospheric parameters. Only small non-LTE effects are predicted for weak Mg I, Mg II, and Fe II lines.

Microturbulence (ξ) has been determied by forcing the Fe II and Ti II abundances to be independent of equivalent width.

TABLE 2

EFFECTIVE TEMPERATURES AND GRAVITIES FROM CALIBRATIONS

HD	13476	87737	46300
Relyea & Kurucz (1978):			
c_o vs $(b-y)_o$	8500,1.0	9500,1.4	9500,1.5
m_o vs $(b-y)_o$	8500,1.0	9500,1.3	9300,1.4
c_o vs m_o	8800,1.3	9600,1.5	9600,1.7
Moon & Dworetsky (1985):			
β vs c_o	9500,1.7	10400,2.2	10200,2.1
Lester, Gray & Kurucz (1986):			
β vs [c_1]	9000,1.2	10000,1.8	10000,1.8
c_o vs $(b-y)_o$	8500,1.0	9400,1.4	9400,1.4
Gray (1992):			
semi-emp. formula	8700, ...	9300, ...	9200, ...
Hγ fits (this paper):			
	8500,1.2	9500,1.9	9500,2.0
	9000,1.5	10000,2.1	10000,2.2
	9500,1.7	10500,2.2	10500,2.3
Mg I/Mg II ioniz.eqm (this paper):			
	8500,1.05	9300,1.5	9300,1.5
	8800,1.5	9500,1.75	9500,1.75
	9000,1.8	9700,2.0	9700,2.0
	9150,2.0	10000,2.4	10000,2.4
Adopted:	8650,1.3	9650,1.95	9800,2.15
with ξ (km s^{-1})	8.0	4.0	4.0

NOTE.—Values of $T_{\rm eff}$ (K), log g (dex) are tabulated.

There are several of these lines (25–40) and of varying strengths for somewhat reliable determinations, but there are too few lines and in too small a spectral range to investigate atmospheric depth or species dependence of the microturbulence. The initial determination of ξ is not self-consistent because ξ is a parameter one may set when generating a model atmosphere using ATLAS9, and this value affects the metal line opacity distribution function. We assumed $\xi = 2.0$ for the initial models, determined the best value for each star from the Fe II and Ti II lines, and then recomputed the model atmospheres with the improved value of ξ. The same value of ξ was found from the improved models from each star such that another iteration was not necessary. Nevertheless, the value of microturbulence should not be critical in this analysis since only weak lines are included in the final, averaged abundances. The use of weak lines also means that radiative damping terms should not be important.

3.3. *Accuracies of the Atmospheric Parameters*

The internal uncertainties in the Hγ profile comparisons can be determined for each parameter ($T_{\rm eff}$ and gravity) by holding the other parameter constant. At constant temperature, log g may vary by ± 0.1 and still reproduce the Hγ line wings adequately; at constant gravity, $T_{\rm eff}$ may vary by about ± 200 K (see Fig. 3 for the sample fits to Hγ in HD 46300). The uncertainties in $T_{\rm eff}$ and log g from ionization equilibrium of magnesium can be determined by allowing a maximum difference between log ϵ(Mg I) and log ϵ(Mg II) of 0.2 (to account for uncertainties in the oscillator strengths or measured equivalent widths). At constant temperature, log g may vary by ± 0.2 dex (HD 13476) or ± 0.3 dex (others), while at constant gravity, $T_{\rm eff}$ may vary by ± 200 K (HD 13476) or ± 250 K (others). The smallest of these uncertainties for each star (thus from the most constrained observable) is plotted as the error bar to the final points in Figure 4.

The derived values of microturbulence have an uncertainty of ± 1 km s^{-1} and are similar to those determined by Aydin (1972) and Rosendahl (1970). In Figure 5*a*, a representative plot of log ϵ(Fe II) versus log (W_λ/λ) for HD 13476 shows that there is no significant trend in abundance with equivalent width as is required in the microturbulence determination. We also have plotted log ϵ(Fe II) versus χ (the lower excitation potential in eV) and wavelength in Figures 5*b* and 5*c*, respectively. The lack of a relationship between abundance and excitation potential suggests that the excitation temperature (= effective temperature in LTE) has been well determined for this star, and the final plot of abundance versus wavelength shows that no systematic variations appear in the continuum placement over the range in spectral energy distribution.

In the previous studies of microturbulence in A supergiant atmospheres, it has been claimed that ξ varies between elemental species and with atmospheric depth. Aydin (1972) found that ξ varies from element to element in the atmospheres of Ia to Ib A supergiants, such that ξ(Fe II) > ξ(Ti II, Cr II) > ξ(Fe I). Values of 5–12 km s^{-1} were derived for the ions (the Ib supergiants tending toward the lower values) and 4–5 km s^{-1} for the Fe I lines. Rosendahl (1970) also found these trends in ξ with species, and claimed the values appear depth-dependent from an examination of lines found at different photospheric levels. One of Rosendhal's stars is HD 13476, for which we have

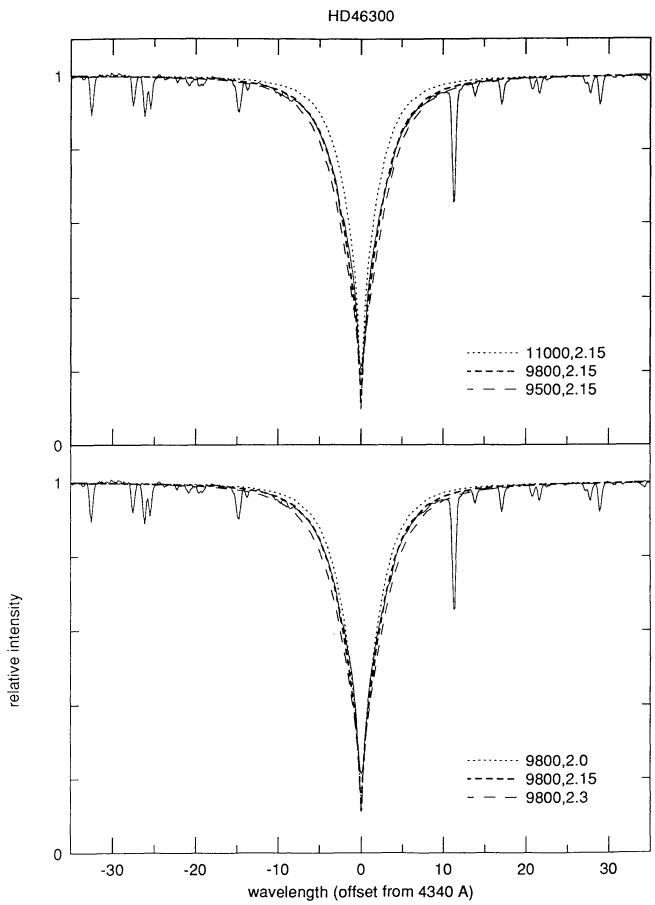

FIG. 3.—Spectrum of the observed Hγ profile for HD 46300 with superposed theoretical profiles generated using BALMER. The atmospheric parameters, $T_{\rm eff}$ and log g, are shown in the lower right corner for each theoretical profile; $\xi = 4.0$ throughout.

determined $\xi = 8 \pm 1$ km s^{-1} (from 25 lines of Fe II and 16 lines of Ti II). This value is in good agreement with his results ξ(Fe II) = 11.6, ξ(Ti II) = 9.3, and ξ(Fe I) = 6.4 km s^{-1} (from 20 Fe II lines, 25 Ti II lines, and 24 Fe I lines) with an estimated uncertainty of about 1 km s^{-1} each. When our improved gf-values are used with Rosendhal's data set, we find no differences in ξ with species, therefore we consider our single value for ξ sufficient and appropriate for an abundance analysis of HD 13476.

In Table 3 we summarize the atmospheric parameters found previously for HD 87737 and HD 46300 to show they agree moderately well with the values determined here (no previous determinations from model atmospheres are available for HD 13476). The atmospheric parameters for HD 87737 derived by Wolf (1971) were found from several spectroscopic indicators using early Kurucz models (without line blanketing). These included the size of the Balmer discontinuity, the equivalent widths of Hγ, Hδ, and Hε, and ionization equilibrium between Mg I and Mg II. Wolf then adopted a depth-dependent microturbulence to account for systematic abundance differences he found between weak and strong lines within a multiplet and the appearance that larger abundances were determined using metal lines formed shortwards of the Balmer jump (which form in higher atmospheric layers). A recent reexamination of Wolf's data by Lobel et al. (1992) using modern Kurucz atmospheres found that a single microturbulence value is sufficient for the abundance analysis (as we have found for HD 13476 above). Lobel et al. also determine slightly different model atmosphere parameters primarily from the method of ionization equilibrium using lines of Fe I and Fe II. The atmospheric parameters determined by Lambert et al. (1989) for HD 87737 are primarily from Strömgren colors and the calibrations by Moon & Dworetsky (1985). The values for $T_{\rm eff}$ for HD 87737

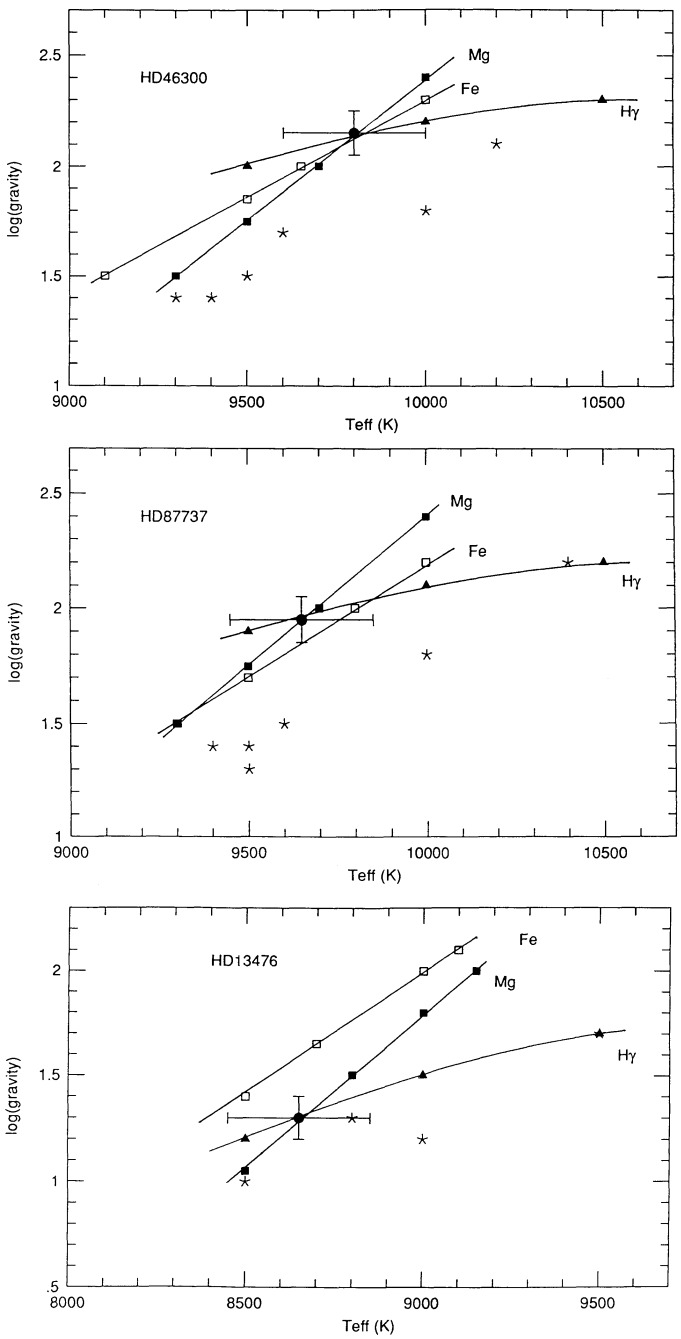

FIG. 4.—Atmospheric parameters, $T_{\rm eff}$ and log g, that reproduce the observed Hγ line profiles (*solid triangles*), and that determine ε(Mg I) = ε(Mg II) (*solid squares*). Atmospheric parameters that yield ε(Fe I) = ε(Fe II) are also indicated (*hollow squares*), as well as the photometric calibrations listed in Table 4 (*five-point stars*). The adopted model atmosphere parameters (*solid circles*) and the estimated uncertainties are marked.

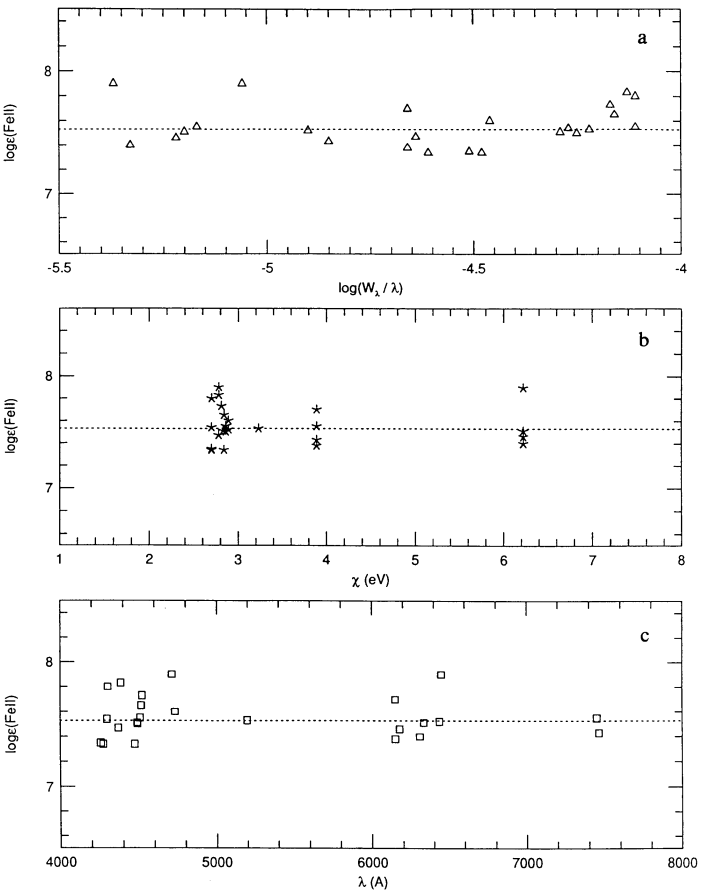

FIG. 5.—Plots of log ϵ(Fe II) vs. equivalent width, excitation potential (χ in eV), and wavelength for HD 13476; log ϵ(Fe II) is marked (*dashed line*). These plots are to show that no significant systematic errors are apparent due to ξ, $T_{\rm eff}$, or the continuum placement, respectively.

and HD 46300 in Table 3 by Przybylski (1969) were determined from ionization equilibrium of Fe I and Fe II lines; the values of gravity for these stars are estimates from Przybylski's determinations of electron pressure, where he used the Balmer jump and equivalent widths of the Balmer lines in each star, and a revised version of the Inglis-Teller formula (see Allen 1973, p. 68). His microturbulence value was determined from a comparison of the Fe II lines to a theoretical curve of growth.

TABLE 3

PREVIOUS DETERMINATIONS OF ATMOSPHERIC PARAMETERS

	$T_{\rm eff}$ (K)	Log g	ξ (km s^{-1})
HD 87737:			
This paper	9650 ± 200	1.95 ± 0.10	4.0 ± 1.0
Wolf (1971)	10400 ± 300	2.05 ± 0.20	2.0 (τ=1.3) to 10.0 (τ=0.0)
Lobel et al. (1992)	10200 ± 370	1.9 ± 0.4	5.4 ± 0.7
Lambert et al. (1989)	10500	2.2	3.0
Przybylski (1969)	9500	1.1	4.6
HD 46300:			
This paper	9800 ± 200	2.15 ± 0.10	4.0 ± 1.0
Przybylski (1969)	9500	1.0	3.6

3.4. *Estimated Effects of Departures from LTE on the Atmospheric Parameters*

The difference in microturbulence between species (particularly betwen Fe I and Fe II) previously reported for the A supergiants has also been reported for the F supergiants, even when modern, accurate oscillator strengths are used (Russell & Bessell 1989; Lyubimkov & Boyarchuk 1983). In the F supergiants, Boyarchuk, Lyubimkov, & Sakhibullin (1985) suggest that the difference is real and is a non-LTE effect caused by a difference in the photoionization temperature and recombination temperature in the line-forming regions. Photoionization is strongly affected by UV radiation from deeper, hotter atmospheric layers, yet recombination processes occur under the local thermal atmospheric temperature. Since most of the iron atoms are in the Fe II state, then an increase in ionization makes little difference to N(Fe II). However, increased ionization has a significant effect on the less abundant Fe I state. Due to overionization, the Fe I state is less populated than determined under the assumption of LTE; thus, for a given equivalent width, a non-LTE calculation yields a larger number of absorbers than an LTE calculation. Estimates of the LTE underabundances due to the overionization of Fe I in the F supergiants are ~0.2 dex (F0 supergiants) to ~0.03 dex (F8 supergiants) for weak lines (Boyarchuk et al. 1985). Since overionization occurs mostly in the upper layers of the atmosphere, then using weak lines with high excitation potentials (i.e., lines that form deeper in the atmosphere) may minimize the effect; also, small changes to weak lines on the linear part of the curve of growth result in only small abundance deviations.

Will departures from LTE cause Fe I to be overionized in the A supergiant atmospheres? Gigas (1986) has determined LTE and non-LTE abundances for iron in Vega (an A0 main sequence star) and finds the LTE Fe I abundance may be underestimated by ~0.3 dex from a weak line (10–80 mÅ) analysis. Unfortunately, this estimate is very sensitive to the assumed values for photoionization and collision cross sections, which are not well known. Gigas finds the non-LTE corrections are also senstive to gravity (due to changes in the collision rates), but are not very temperature sensitive. This may imply that the corrections determined for the F0 supergiants approximate those for the late A supergiants (about 0.2 dex from Boyarchuk et al. 1985) although this is a large extrapolation. It is not clear what to expect for corrections to the Fe I abundances in the early A supergiants, although at least 0.2–0.3 dex seems likely even for weak lines with high excitation potentials. Thus, the uncertainty in the Fe I abundances derived here due to neglected non-LTE effects make Fe I an unreliable abundance indicator, especially for the ionization equilibrium determinations of the atmospheric parameters.

Gigas (1988) has also determined LTE and non-LTE abundances of magnesium from Mg I and Mg II in Vega. Similar to iron, most of the magnesium atoms are in the Mg II state, and Mg I is slightly overionized by the radiation field. Nevertheless, Gigas finds that the occupation numbers for Mg I and Mg II for most levels are very close to the LTE values in the line-forming regions. Thus, non-LTE effects are not very pronounced for magnesium in the main sequence A stars. The Mg I corrections are slightly sensitive to surface gravity, but not to temperature, and they are not as sensitive as Fe I to the assumed photoionization and collision rates. Thus, we assume non-LTE corrections to Mg I line abundances in A supergiants are small.

The non-LTE studies (Gigas 1986, 1988; Boyarchuk et al. 1985) find no significant departures from LTE for either Mg II or Fe II throughout the atmosphere except in the highest layers where the corrections are still small (<0.1 dex). Therefore, Mg II and Fe II lines are considered reliable abundance indicators for the A supergiants. A rigid insistence on ionization balance to determine atmosphere parameters may be prone to systematic errors, but calculations using Mg I and Mg II lines should be somewhat reliable and have been used extensively in this analysis. The Fe I and Fe II abundances are still compared for ionization balance, but only as a check on the resultant parameters.

Other non-LTE effects may be important in the analysis of A supergiant abundances. For example, Kudritzki (1973) has shown that the temperature stratification (and therefore the overall structure) of an A0 Ia-type supergiant atmosphere may be subject to non-LTE effects. Kudritzki has also shown that departures from LTE can cause an overpopulation of the $n = 1, 3$ levels in the hydrogen atoms, but an underpopulation of the $n = 2$ level, which affects the hydrogen line strengths and height of the Balmer discontinuity. Unfortunately, it is difficult to estimate the magnitude of this effect on our abundance analysis from Kudritzki's paper. To estimate the effect we looked at a similar non-LTE analysis by Frandsen (1974) for A0 stars; he estimates that at $\log g = 2.0$, the Hβ Strömgren index (which measures the strength of the Hβ line) changes by $\sim$10%. From the photometric calibrations discussed above, this would correspond to a change in $\log g$ of less than ± 0.2 or a change in $T_{\rm eff}$ of less than ± 200 K. These are acceptable uncertainties in the atmospheric parameters, and one might expect the weaker Hγ line to be even less affected. Frandsen also states that when $\log g < 2.0$ a considerable portion of the Balmer lines form in layers where departures from LTE are significant. Therefore, the uncertainties in the models are most likely more intrinsic than just adjustments to $T_{\rm eff}$ and gravity, since the temperature and pressure stratifications are affected which changes the continuous flux distribution. Ideally, non-LTE and line-blanketed model atmospheres should be used for a quantitative abundance analysis of the A supergiants; however, such models are very difficult to generate, and for the Ib-type supergiants the non-LTE effects in the atmospheres do not seem large.

The helium abundance can also have an effect on the atmospheric parameters of A-F–type stars that mimic changes in gravity (Kudritzki 1973; Böhm-Vitense 1979; Strömgren, Olsen, & Gustafsson 1982). An increase in the helium abundance changes the mean molecular weight of a column of gas in the atmosphere, which modifies the pressure stratification as a function of optical depth. The increase in the mean molecular weight also affects the continuous absorption coefficient, κ_c, by decreasing the amount of opacity per gram of gas, thus placing $\kappa_c = 1$ deeper in the atmosphere. This affects the spectral energy distribution such that the hydrogen discontinuities are larger and the hydrogen lines are stronger. These changes in the spectrum are the same as those obtained by increasing the gravity. As an example, increasing the helium fraction to 0.5 (from the normal fraction of 0.1) in a 10,000 K A supergiant atmosphere can increase the equivalent width of Hγ by about a factor of 2 (Humphreys et al. 1991). If one tried to estimate the gravity from this line without considering the helium enrichment, the estimate will be too large by about 0.3 dex. However, the effects of the helium abundance are not quite as striking at higher gravities where electron densities are higher, such as in the Iab and Ib stars in this analysis. Also in this analysis of normal A supergiants, we do not expect such a significant change in the helium fraction; if these stars have nearly first dredge-up abundances then the helium fraction increases by only 10% (Maeder & Meynet 1988).

4. ABUNDANCE RESULTS

Abundance results for each spectral line are presented in Table 4, along with the equivalent width (in mÅ), adopted oscillator strength, and multiplet number. An attempt has been made to remove any faulty or questionable equivalent width data. Lines that have been removed include exceedingly weak ($W_\lambda < 5$ mÅ) and strong ($W_\lambda > 400$ mÅ) lines, and those significantly blended with other elements. Lines from particularly crowded spectral regions that are blended with the wings of nearby lines have also been excluded if the computed abundances were greater than 2 σ from the mean—this also excludes all lines that occur well into the wings of Balmer lines.

Final abundance results are presented in Table 5 as unweighted average abundances per species. Abundances are given on the usual scale, $\epsilon(x) = N(x)/N(\mathrm{H})$, where $\log \epsilon(\mathrm{H}) = 12.0$, and $[x] = \log \epsilon(x)_* - \log \epsilon(x)_\odot$. The adopted solar abundances are the meteoritic abundances discussed by Anders & Grevesse (1989), with three exceptions. For oxygen, we chose the Anders & Grevesse solar photospheric abundance, and the adopted solar carbon and nitrogen abundances are the recent photospheric abundance determinations by Grevesse et al. (1991) and (1990), respectively. Only weak lines have been used to compute the averages (the number of lines averaged are included in Table 5). Weak lines are defined as those where a change in ξ of ± 1.0 km s^{-1} yields a change in the derived abundance of less than 0.1 dex. Strong lines in Table 4 that do not meet this criterion are marked in italics and are not included in the final averages. Important abundance ratios and the sums [(C+N+O)/Fe] are listed in Table 6, and can be compared to the predicted results from Maeder & Meynet (1988).

Estimated abundance uncertainties per species are listed in Table 7, including uncertainties due to the atmospheric parameters ($T_{\rm eff}$, $\log g$), the microturbulence, and the line-to-line scatter (σ). When less than five lines are averaged, σ is probably not a true indicator of the possible error in the abundance. Also, since only weak lines have been used to calculate the final abundances, then the uncertainties due to a 1 km s^{-1} change in microturbulence are all less than 0.1 dex (the weak line criterion defined above). Many elemental abundances are not sensitive to the adopted atmospheric parameters. An increase in temperature by 200 K increases the abundances of many species by less than 0.1 dex (N I, O I, Mg II, Cr II, Fe II) and the other species change by less than 0.2 dex (C I, Mg I, Ti II, Fe I); an exception is $\log \epsilon$(Fe I) in HD 13476, where the abundance increases by 0.25 dex. The less luminous A0 Ib supergiants have abundances that are mostly insensitive to gravity; increasing $\log g$ by 0.2 dex changes the abundances by only 0.03–0.13 dex. For the luminous supergiant, HD 13476, most species are similarly insensitive to gravity, except for the abundances derived from lines of C I, Mg I, and Fe I which decrease by about 0.2 dex with this increase in gravity. There is also an uncertainty in the abundances due to the accuracy of the measured equivalent widths. We estimate that the widths are accurate to within 15%, which corresponds to an uncertainty in the abundances of less than 0.1 dex for weak lines.

TABLE 4

SINGLE SPECTRAL LINES OBSERVED

Wavel. (Å)	Mult.	log *gf*	Ref	χ (eV)	HD 13476		HD 87737		HD 46300	
					W_λ	log ε	W_λ	log ε	W_λ	log ε
C I										
7113.18	(26)	−0.76	(1)	8.65	12	8.26	<10	<8.46	<10	<8.46
7115.19	(25.02,26)	−0.92	(1)	8.64	10	8.23	<10	<8.62	<10	<8.62
7116.99	(25.02)	−0.91	(1)	8.65	17	8.56	<10	<8.57	<10	<8.61
7119.67	(25.02)	−1.15	(1)	8.64	13	8.68	<10	<8.85	<10	<8.85
9061.48	(3)	−0.34	(1)	7.48	...	...	90	8.33	...	...
9062.53	(3)	−0.45	(1)	7.48	...	...	86	8.41	...	...
9078.32	(3)	−0.58	(1)	7.48	184	8.56	58	8.27	46	8.13
9088.57	(3)	−0.42	(1)	7.48	240	8.67	82	8.34	63	8.16
9094.89	(3)	0.16	(1)	7.49	392	*8.97*	175	*8.60*	145	8.32
9111.85	(3)	−0.29	(1)	7.49	240	8.55	81	8.21	60	8.00
N I										
7423.63	(3)	−0.69	(2)	10.33	95	8.77	74	8.95	59	8.78
7442.28	(3)	−0.40	(2)	10.33	164	8.95	118	*9.19*	95	8.93
7468.29	(3)	−0.21	(2)	10.34	214	9.09	152	*9.45*	119	*9.09*
8184.80	(2)	−0.29	(2)	10.33	250	*9.56*	...	...	115	*9.17*
8187.95	(2)	−0.29	(2)	10.33	251	*9.57*	...	...	120	*9.24*
8200.31	(2)	−1.00	(2)	10.33	...	...	...	...	38	8.87
8210.64	(2)	−0.68	(2)	10.33	128	8.62	...	...	62	8.43
8216.28	(2)	0.09	(2)	10.34	358	*9.09*	...	...	174	*8.70*
8223.07	(2)	−0.29	(2)	10.33	218	8.69	...	...	110	*8.49*
8242.34	(2)	−0.26	(2)	10.34	216	8.65	...	...	107	*8.44*
8629.24	(8)	0.08	(2)	10.69	269	*8.84*	167	*8.88*	134	*8.57*
8703.24	(1)	−0.34	(2)	10.33	279	*9.08*	198	*9.42*	156	*8.99*
8711.69	(1)	−0.24	(2)	10.33	306	*9.12*	204	*9.39*	161	*8.94*
8718.82	(1)	−0.35	(2)	10.34	258	*8.99*	178	*9.22*	136	*8.82*
8728.88	(1)	−1.04	(2)	10.33	91	8.78	74	8.93	47	8.64
O I										
6155.99	(10)	−0.67	(1)	10.74	42	8.68	50	8.96	41	8.83
6156.78	(10)	−0.45	(1)	10.74	82	8.85	70	8.87	61	8.88
6158.19	(10)	−0.31	(1)	10.74	99	8.84	80	8.97	71	8.87
7156.80	(38)	0.26	(3)	12.73	16	8.60	31	8.99	30	8.96
Mg I										
4702.98	(11)	−0.37	(3)	4.35	43	7.59	...	...	...	...
5167.32	(2)	−0.86	(3)	2.71	121	7.56	45	7.62	33	7.46
5172.68	(2)	−0.38	(3)	2.71	174	7.37	70	7.43	56	7.28
5183.60	(2)	−0.16	(3)	2.72	193	7.25	86	7.37	74	7.26
Mg II										
4390.59	(10)	−0.53	(4)	10.00	126	7.63	85	7.52	78	7.44
4427.99	(9)	−1.21	(4)	10.00	26	7.33	31	7.48	26	7.38
4433.99	(9)	−0.91	(4)	10.00	36	7.20	50	7.47	40	7.33
4739.59	(18)	−0.66	(4)	11.57	30	7.77	...	...	...	...
7877.13	(8)	0.39	(4)	10.00	149	7.34	115	7.55	98	7.31
7896.37	(8)	0.65	(4)	10.00	221	*7.62*	178	*8.25*	177	*8.25*
Ti II										
4287.89	(20)	−2.02	(5)	1.08	113	5.15	20	4.91	13	4.77
4290.22	(41)	−1.12	(5)	1.16	271	*5.21*	68	4.76	48	4.59
4294.10	(20)	−1.11	(5)	1.08	267	*5.11*	77	4.79	55	4.62
4300.05	(41)	−0.77	(5)	1.18	352	*5.59*	112	4.88	87	4.67
4301.93	(41)	−1.16	(5)	1.16	207	4.84	41	4.47	29	4.35
4307.90	(41)	−1.29	(5)	1.16	227	5.09	69	4.94	51	4.80
4312.86	(41)	−1.16	(5)	1.18	204	4.84	55	4.66	41	4.55
4316.81	(94)	−1.42	(5)	2.05	48	4.72	...	...	...	...
4374.83	(93)	−1.29	(5)	2.06	...	...	16	4.66	11	4.54
4395.03	(19)	−0.66	(5)	1.08	383	*5.61*	...	...	...	...
4468.49	(31)	−0.60	(5)	1.13	302	*4.88*	89	4.42	67	4.27

TABLE 4—*Continued*

Wavel. (Å)	Mult.	log *gf*	Ref	χ (eV)	HD 13476		HD 87737		HD 46300	
					W_λ	log ϵ	W_λ	log ϵ	W_λ	log ϵ
4501.27	(31)	−0.75	(5)	1.12	289	*4.90*	79	4.46	59	4.31
4529.47	(82)	−2.03	(5)	1.57	82	5.28	...	...	...	...
4708.66	(49)	−2.21	(5)	1.24	37	4.82	...	...	...	...
4779.99	(92)	−1.37	(5)	2.05	98	5.03	...	...	...	...
5185.90	(86)	−1.35	(5)	1.89	87	4.82	29	4.89	17	4.69
5188.70	(70)	−1.21	(5)	1.58	151	4.84	34	4.65	39	4.79
Cr II										
4224.85	(162)	−1.06	(6)	5.33	69	5.72	...	...	...	...
4252.62	(31)	−1.86	(6)	3.86	84	5.67	...	...	...	...
4269.28	(31)	−2.02	(6)	3.85	66	5.69	...	...	...	...
4275.57	(31)	−1.47	(6)	3.86	71	5.19	...	...	...	...
4284.21	(31)	−1.70	(6)	3.85	...	...	46	5.58	33	5.45
Fe I										
4235.94	(152)	−0.32	(7)	2.43	28	7.33	...	...	...	...
4238.82	(693)	−0.23	(7)	3.40	36	7.99	...	...	...	...
4260.48	(152)	0.08	(7)	2.40	56	7.25	...	...	...	...
4282.41	(71)	−0.78	(7)	2.18	...	...	15	7.88	14	7.86
4383.55	(41)	0.21	(7)	1.48	...	...	59	7.21	43	7.03
4494.57	(68)	−1.14	(7)	2.20	30	8.01	...	...	...	...
4707.28	(554)	−1.08	(8)	3.24	8	8.03	...	...	...	...
4736.78	(554)	−0.75	(7)	3.21	15	7.96	...	...	...	...
8688.63	(60)	−1.20	(7)	2.18	32	7.89	...	...	...	...
Fe II										
4258.16	(28)	−3.40	(8)	2.70	132	7.35	...	...	...	...
4273.32	(27)	−3.34	(8)	2.70	140	7.34	...	...	...	...
4296.57	(28)	−3.01	(8)	2.70	232	*7.54*	121	*7.60*	96	7.36
4303.17	(27)	−2.49	(8)	2.70	337	*7.81*	181	*7.80*	141	*7.39*
4314.29	(32)	−3.48	(4)	2.68	...	...	85	7.62	60	7.41
4319.72	(220)	−1.76	(4)	7.84	...	...	20	7.83	...	...
4369.40	(28)	−3.67	(8)	2.78	100	7.47	49	7.46	41	7.41
4385.38	(27)	−2.57	(8)	2.78	326	*7.83*	160	*7.75*	125	*7.30*
4472.92	(37)	−3.43	(8)	2.84	110	7.34	59	7.38	47	7.29
4489.19	(37)	−2.97	(8)	2.83	222	*7.51*	115	*7.54*	87	7.29
4491.40	(37)	−2.70	(8)	2.86	259	*7.50*	134	*7.53*	103	*7.21*
4508.28	(38)	−2.21	(8)	2.86	333	*7.55*	187	*7.87*	146	*7.27*
4515.34	(37)	−2.48	(8)	2.84	311	*7.65*	167	*7.81*	128	*7.29*
4520.23	(37)	−2.60	(8)	2.81	308	*7.73*	...	...	...	...
4522.63	(38)	−2.03	(8)	2.84	412	*8.04*	...	...	...	...
4713.18	(26)	−4.93	(4)	2.78	20	7.90	...	...	...	...
4731.44	(43)	−3.36	(8)	2.89	163	7.60	...	...	...	...
5160.82	(167)	−2.64	(4)	5.57	...	...	30	7.75	25	7.70
5169.03	(42)	−0.87	(8)	2.89	...	...	...	...	285	*8.10*
5197.57	(49)	−2.10	(8)	3.23	315	*7.53*	169	*7.71*	133	*7.23*
5362.86	(48)	−2.33	(9)	3.20	...	...	...	...	108	*7.14*
5991.38	(46)	−3.74	(8)	3.15	...	...	...	...	29	7.56
6147.74	(74)	−2.61	(8)	3.89	133	7.38	72	7.41	54	7.25
6149.24	(74)	−2.92	(8)	3.89	134	7.70	69	7.69	56	7.59
6175.16	(200)	−1.98	(8)	6.22	37	7.46	39	7.71	29	7.58
6179.38	(163)	−2.81	(8)	5.57	...	...	21	7.81	14	7.66
6305.32	(200)	−2.04	(4)	6.22	29	7.40	...	...	...	...
6331.97	(199)	−1.98	(4)	6.22	40	7.51	40	7.74	22	7.44
6432.65	(40)	−3.74	(8)	2.89	80	7.52	...	...	...	...
6446.43	(199)	−2.16	(8)	6.22	56	7.90	...	...	...	...
7449.34	(73)	−3.31	(4)	3.89	50	7.55	24	7.50	19	7.44
7462.38	(73)	−2.73	(4)	3.89	106	7.43	66	7.58	51	7.45

NOTE.—Weak lines only have been used in the averaged abundances (see text). Abundances that are *not* used in the averages are marked in italics.

REFERENCES.—(1) Opacity Project (Hibbert et al. 1991a, 1992); (2) Zhu et al. 1989; (3) Wiese & Martin 1980; (4) Kurucz 1990; (5) Martin et al. 1988; (6) Sigut & Landstreet 1990; (7) O'Brian et al. 1991; (8) Fuhr et al. 1988; (9) Fuhr et al. 1981.

TABLE 5

ABUNDANCE RESULTS

Elem	Sun[a]	HD 13476			HD 87737			HD 46300		
	logϵ	logϵ	[ϵ]	(#)	logϵ	[ϵ]	(#)	logϵ	[ϵ]	(#)
C I	8.60	8.50	−0.10	(7)	8.31	−0.29	(5)	8.15	−0.45	(4)
N I	8.00	8.79	+0.79	(7)	8.94	+0.94	(2)	8.73	+0.73	(5)
O I	8.93	8.74	−0.19	(4)	8.95	+0.02	(4)	8.89	−0.04	(4)
Mg I	7.58	7.44	−0.14	(4)	7.47	−0.11	(3)	7.33	−0.25	(3)
Mg II	7.58	7.45	−0.13	(5)	7.51	−0.07	(4)	7.37	−0.21	(4)
Ti II	4.93	4.94	+0.01	(10)	4.71	−0.22	(12)	4.58	−0.35	(12)
Cr II	5.68	5.57	−0.11	(4)	5.58	−0.10	(1)	5.45	−0.23	(1)
Fe I	7.51	7.78	+0.27	(7)	7.55	+0.04	(2)	7.45	−0.06	(2)
Fe II	7.51	7.52	+0.01	(15)	7.62	+0.11	(12)	7.44	−0.07	(14)

[a] Adopted solar abundances are the meteoritic abundances discussed by Anders & Grevesse 1989, except for oxygen which is the photospheric abundance discussed. Solar carbon and nitrogen abundances are the more recently determined photospheric abundances by Grevesse et al. 1990, 1991.

4.1. *Mg and Fe*

For all three stars, the final abundances for magnesium are an unweighted average of Mg I and Mg II, while the final values for iron are taken only from the Fe II abundances. In general, the abundances of iron and magnesium are near solar, and this is encouraging because it implies that non-LTE corrections may be small.

Abundances from Mg I lines are sensitive to temperature and gravity, making this element particularly sensitive to the ionization balance in the determination of the atmospheric parameters. For the A0 Ib stars, the abundances from Mg I and Mg II agree to within 0.2 dex over a range of about 500 K (at gravities that also fit the Hγ profiles); the best model has been chosen where ϵ(Mg I) ~ ϵ(Mg II). Coincidentally, the abundances derived from Fe I and Fe II are found to be the same to within 0.1 dex for these models, although the Fe I abundances were derived from only two lines in these two stars with a very large line-to-line scatter (~ ±0.35 dex!). This scatter could not be traced to the measured equivalent widths, unrecognized blends, or erroneous *gf*-values. This same scatter was also found for the seven Fe I lines used to determine the abundances in HD 13476, where all seven lines are different from the two used for the above stars. There is no clear trend with excitation potential, although the scatter may be due to departures from LTE. In HD 13476, the abundances from Mg I and Mg II agree to within 0.2 dex over a smaller range of only 300 K because Mg I is more sensitive to the atmospheric parameters.

TABLE 6

ABUNDANCE RATIOS

ratio	HD 13476	HD 87737	HD 46300	MM[b]
[C/Fe][a]	−0.11	−0.46	−0.34	−0.14
[N/Fe][a]	+0.78	+0.78	+0.83	+0.46
[O/Fe][a]	−0.20	−0.15	+0.07	−0.04
[N/C]	+0.89	+1.24	+1.17	+0.60
[N/O]	+0.98	+0.93	+0.76	+0.50
[C+N+O/Fe][a]	+0.03	0.00	+0.14	0.00

[a] Log ϵ(Fe) = log ϵ(Fe II) only.

[b] Predicted abundance ratios for a 9 $M_\odot$ star after first dredge-up by Maeder & Meynet 1988.

Our derived abundances of iron and magnesium in HD 87737 can be compared to other detailed abundance analyses. Lambert et al. (1989) found [Fe I/H] ~ +0.2 and [Fe II/H] ~ +0.3 from two and three spectral lines, respectively. Using their Fe II equivalent width measurements with our atmospheric parameters increases the abundance they report to [Fe II/H] ~ +0.5, which is about 0.4 dex larger than that determined from our 12 weak lines. Since we have not observed any of their lines we cannot check their equivalent widths. We note however that their lines are all stronger than would be used in this analysis, thus there may be no significant disagreement between our results. Lobel et al. (1992) determine [Fe/H] = +0.14 ± 0.10 from a reexamination of Wolf's (1971) data which includes 47 Fe I and 71 Fe II lines. We have computed abundances from the Wolf data set using our atmospheric parameters and found some disagreements which could be traced primarily to the oscillator strengths (their equivalent measurements are within ~15% of ours). Using our oscillator strengths, the iron abundance calculated from their lines is in very good agreement with ours. For Fe I, we calculate the iron abundance from only two lines, and our results differ by 0.7 dex between the two lines; the Lobel et al. results imply that the lower abundance we derived from λ4383 is more likely correct (even though this transition has the lower excitation potential and may be more subject to non-LTE effects discussed in § 3.4). Perhaps the λ4282 line is blended with an unidentified element and should not be considered a reliable abundance indicator.

To determine the magnesium abundance in HD 87737, Lambert et al. (1989) used only the Mg II λ4390 line (they also report a Mg I line at λ4351, but this is likely a misidentification of the strong Fe II line at that wavelength). They determine [Mg II/H] ~ +0.2 from this line (similar *gf*-value) which is about 0.25 dex larger than that determined here. When our atmospheric parameters are adopted, their abundance decreases to +0.1 dex, and the remaining difference is due to their equivalent width measurement which is about 15% larger. Wolf (1971) determined the magnesium abundance for HD 87737 as [Mg/H] = +0.4 from the average of three Mg I and seven Mg II lines. Using our atmospheric parameters, that abundance is reduced to only +0.2 dex. The only lines in common between their analysis and ours are for Mg II λ4390, λ4428, and λ4434 (similar *gf*-values) for which Wolf's equiva-

TABLE 7

ESTIMATED UNCERTAINTIES

Elem	ΔT_{eff} =+200K		Δlog g=+0.2		$\Delta\xi$=−1 km s^{-1}		σ(line scatter)	
	87737	13476	87737	13476	87737	13476	87737	13476
C I	+0.10	+0.20	−0.07	−0.17	+0.04	+0.03	0.07	0.15
N I	+0.07	+0.10	−0.04	−0.09	+0.09	+0.03	0.01	0.13
O I	+0.03	+0.06	−0.03	−0.07	+0.05	+0.01	0.02	0.11
Mg I	+0.18	+0.20	−0.13	−0.24	+0.07	+0.03	0.11	0.15
Mg II	+0.02	+0.01	−0.01	−0.01	+0.10	+0.05	0.03	0.20
Ti II	+0.14	+0.20	−0.03	−0.10	+0.07	+0.03	0.18	0.17
Cr II	+0.05	+0.07	+0.03	−0.01	+0.05	+0.01	0.00	0.22
Fe I	+0.16	+0.25	−0.10	−0.21	+0.04	+0.01	0.34	0.30
Fe II	+0.02	+0.05	+0.05	+0.02	+0.07	+0.02	0.15	0.17

NOTE.—Uncertainties for HD 87737 ~ HD 46300 [except σ(N I) = 0.15].

lent widths are about 25% larger than ours, thus we expect their W_λ measurements account for the remaining difference.

4.2. *CNO*

The carbon abundances have been determined from multiplet lines near λ9100 and λ7115. Both wavelength regions required the removal of telluric features; imperfect cancellations of these features often degrade the signal-to-noise of the resultant spectra. The λ9100 lines have good equivalent widths for an abundance analysis in the A0 stars (shown in Fig. 1*e* for HD 46300), and even some of these lines in HD 13476 meet the weak line requirement for this analysis. The λ7115 lines can be measured only in the cooler star HD 13476, and even there they are extremely weak as seen in Figure 2. We have estimated upper limits to the λ7115 lines in the remaining two A0 Ib stars; the resultant abundance constraints are in agreement with the abundances calculated from the λ9100 lines and for HD 87737 are similar to the upper limits set by Lambert et al. (1989). The departures from LTE for these C I lines have been calculated by Stürenberg & Holweger (1990) and Takeda (1993) for Vega. The non-LTE corrections to the weak λ7115 lines are less than 0.05 dex, but the corrections are much larger for the strong lines of λ9100, for example, −0.3 dex for the lines at 9111 and 9088 Å ($W_\lambda \sim 60$ mÅ in Vega). These corrections may be larger at lower gravities, but no predictions are given. For HD 13476, the abundance derived from both multiplets are very similar (except for the very strong lines) suggesting that departures from LTE may be more similar between these multiplets than determined for Vega.

The oxygen abundances have been derived from the three weak lines near λ6158, and the weak line at 7156 Å (as shown in Figures 1*a* and 2, for HD 46300). The four lines give consistent abundances for each program star. The oxygen abundance derived by Lambert et al. (1989) for HD 87737 is [O/H] = +0.2, which is larger than our determination but was calculated from only a single O I line at 6158 Å. Their W_λ for this line is similar to our measurement, so that when our atmospheric parameters are adopted the same oxygen abundance is calculated. Baschek, Scholz, & Sedlmayr (1977) determined that non-LTE effects on the level populations of the O I atom are largest at T_{eff} = 10,000 K, and the effects increase with decreasing gravity. They estimate the theoretical equivalent widths from an LTE analysis can be 50% less than those from a non-LTE analysis for a given oxygen abundance in an atmosphere where T_{eff} = 10,000 K, log g = 1.0, and ξ = 0 km s^{-1}. The underestimate is dramatically reduced to 15% when either log g = 4.0 or T_{eff} = 7500 K. In this analysis we tried reducing the equivalent widths by 30% to estimate the non-LTE corrections; this reduction should be appropriate since the stars in this analysis (HD 46300 and HD 87737) have higher gravities than Baschek et al.'s 10,000 K example, or (for HD 13476) T_{eff} is closer to their 7500 K example. The results were that the oxygen abundances were reduced by 0.2 (HD 13476) to 0.3 dex.

Nitrogen abundances have been determined from lines of four near-infrared multiplets. The wings of the Paschen lines near λ8700 make some lines from multiplet 1 unusable (see Fig. 1*e* for HD 46300), and the telluric divisions near λ8200 had to be done very carefully to recover the spectral lines with good signal-to-noise (see Fig. 1*d*). The abundances derived from the different multiplets agree very well. There is a slight hint of a trend between line strength and abundance as seen in Figure 6, although it is not significantly larger than the uncertainties in the abundances (shown by the error bar). As a precaution, we also tested the effects of the damping coefficients on the nitrogen abundances; the radiative coefficients were determined from the adopted oscillator strengths and Stark widths were adopted from the critical review by Konjevic & Roberts (1970). Adjusting the radiative and Stark coefficients had no significant effect on the abundances (<0.01 dex). For HD 87737, the LTE abundance derived by Lambert et al. (1989) ([N/H] ~ +1.0) is similar to ours and was derived from weak lines where their equivalent widths are within 5% of ours. Non-LTE corrections to the N I line abundances in the atmosphere of Vega have been estimated by Takeda (1993) using a very detailed N I model atom (119 terms and 2119 transitions). He finds corrections of about −0.3 dex for all lines when a solar metallicity model is adopted. However, for a model with 1/10 solar metallicity, the corrections increase to −0.5 to −0.9 dex. There are no predictions of how these corrections scale with a decrease in gravity. Lambert et al. (1989) attempted an estimate of the non-LTE correction to nitrogen in the atmosphere of HD 87737 using a very simple model atom and methods described by Luck & Lambert (1985). Similar to Takeda's Vega example, they found that departures from LTE could enhance the N I lines in the A supergiant atmosphere. The non-LTE corrections for weak lines were predicted to be near zero, but corrections as large as −1.0 dex were found for the strongest lines. This astonishing result is questionable due

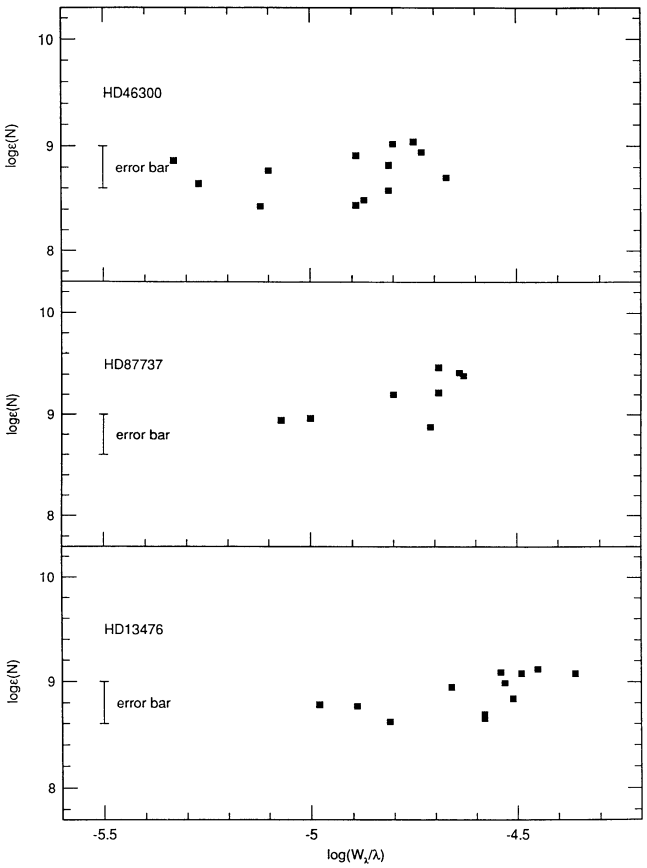

FIG. 6.—Plot of N I abundances vs. log (W_λ/λ) for each star. There is a slight trend in abundance with line strength although it is not significant within the estimated uncertainties as shown by the error bar.

to the simplified N I model atom they used and uncertainties in the atomic data (such as photoionization and collision cross-section rates). In the study of a high Galactic-latitude A7 supergiant ([Fe/H] ~ -0.35), Luck et al. (1990) have also suggested that non-LTE effects can be large, particularly within a single multiplet. They report that some of the N I lines near λ8710 are too strong such that the whole multiplet could not be fitted with a single nitrogen abundance by spectrum synthesis in LTE. The N I abundances derived here do not clearly corroborate their results since the mean abundances from the strong and weak lines are similar to within about 0.3 dex. Thus, non-LTE effects cannot be ruled out as the source of the extreme nitrogen enhancements calculated here for A supergiants. We note, however, that (1) we include only weak lines, (2) we see no significant trends in the nitrogen abundance with line strength (considering the estimated uncertainties), and (3) we see no trends in abundance between multiplets.

4.3. *Other Metals*

Other elemental abundances determined in all three stars include Ti II and Cr II which are between 0.0 and 0.3 dex below solar. Unfortunately, the Cr II abundances in the A0 Ib stars are based on only one line each. A Sc II abundance has also been determined for HD 13476 based on two lines, λ4320.8 ($W_\lambda = 178$ mÅ) and λ4374.5 ($W_\lambda = 174$ mÅ). These lines yield a mean abundance of 3.36 ± 0.08, thus [Sc II] $= +0.27$, which is not significantly different from solar. This abundance is very sensitive to temperature ($\Delta T_{\rm eff} = +200$ K yields $\Delta \log \epsilon$(Sc II) $= +0.27$), but relatively insensitive to gravity and microturbulence ($\Delta \log g = +0.2$ and $\Delta\xi = +1$ km s^{-1} yield $\Delta \log \epsilon$(Sc II) ≤ -0.08).

5. DISCUSSION

The abundances determined here for the three normal A supergiants are shown in Figure 7 relative to solar. We find the metal abundances are near solar for each supergiant, as may be expected for normal Population I stars. Since the progenitor stars are more massive than the Sun, one may expect some small enrichment in the metal abundances due to Galactic chemical evolution; however, no certain enrichments are found.

The abundances of carbon, nitrogen, and oxygen are different from solar in most cases. The nitrogen abundances are extremely enriched ($\langle$[N]$\rangle \sim +0.8$), and the carbon and oxygen abundances are near solar or slightly depleted (between 0.0 to -0.4 dex). This abundance signature suggests CNO cycling, where the surface abundances have been mixed with CNO-processed gas. If CNO-cycling is responsible, then the sum of the CNO nuclei will not have changed from the value for its initial composition. We find [(C+N+O)/Fe] between 0.00 and 0.14 for the three A supergiants (see Table 6), which is within the uncertainties of the analysis to assume the total number of atoms has not changed from an initially solar composition.

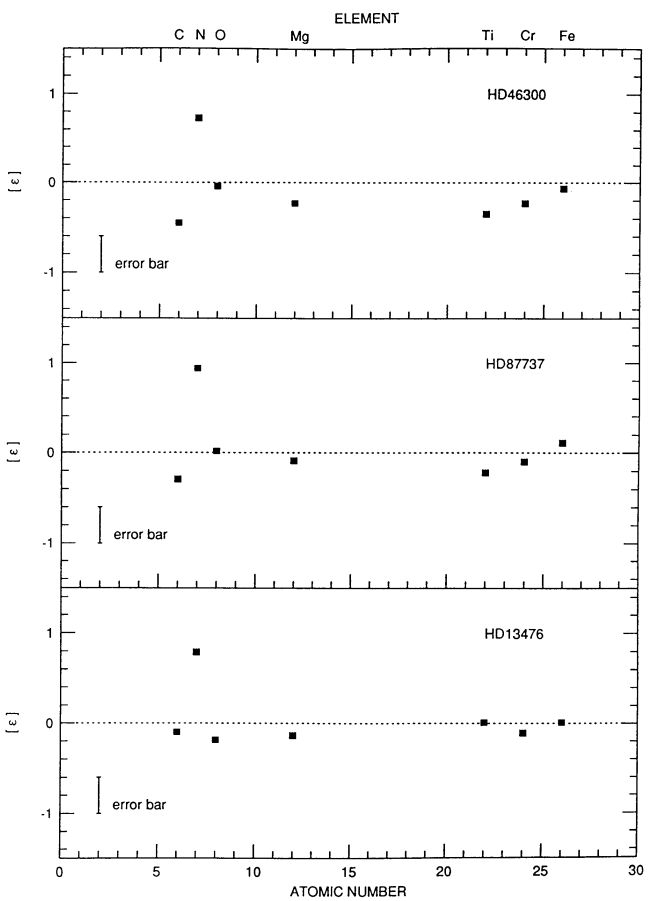

FIG. 7.—Abundances determined in this analysis for the three A supergiants relative to solar.

The three stars analyzed have masses between about 8 and 12 $M_\odot$ from standard calibrations. For these stars, significant mixing of CN-cycled material is predicted at the stellar surface after the first dredge-up, with only a very small amount of ON-cycled gas (the CN-cycle is driven more efficiently at lower temperatures than the ON-cycle, thereby reaching near equilibrium before significant ON-cycling begins). Predictions by Maeder & Meynet (1988, hereafter MM) for a 9 $M_\odot$ star after first dredge-up are approximately [N] = +0.46, [C] = −0.14, and [O] = −0.04, yielding [N/C] = 0.6 and [N/O] = 0.5. These predictions are about the same for a 12 $M_\odot$ star, except [N] = +0.55. The MM models include a treatment for mass loss and convective overshoot and assume Galactic metallicities and interstellar CNO. The interstellar CNO abundances are different from solar; however, we are only interested in the change in the abundances after the first dredge-up mixing event, which presumably are independent of the initial abundance values. First dredge-up abundances calculated by Becker & Iben (1979) are very similar to those by MM, even though the Becker & Iben models do not include mass loss or overshoot. The MM abundances are also very similar to those from the most recent grid of evolution models by Schaller et al. (1992) which improve on the MM models by using new radiative opacities and improved physical parameters (e.g., nuclear reaction rates).

The three A supergiants have [N/C] and [N/O] ratios that are larger than predicted by about 0.3–0.6 dex (as listed in Table 6), which may indicate mixing of an excess of CNO-cycled gas. Luck & Lambert (1985) have also suggested the F-K supergiants have CNO abundances that indicate excess mixing from the first dredge-up predictions. There are several possible mechanisms for additional mixing of processed gas in these stars; these include greater mass loss of the outer hydrogen envelope, meridional mixing near the main sequence, deeper convective zones during dredge-up, or a change in a key evolution parameter (e.g., the overshoot parameter). Further evidence for additional mixing comes from recent CNO abundances determined for B supergiants by Gies & Lambert (1992), where the surface abundances of some stars appear to have been exposed to partial mixing of CN-cycled elements early in their evolution.

Another critical test of the presence of CNO-processed gas is to check whether the N abundance scales with the sum (C+O). During CNO-cycling, the increase in the number of N atoms will equal the sum of the decreases in the number of carbon atoms (from CN-cycling) and oxygen atoms (from ON-cycling). In Figure 8 we plot N versus (C+O), but corrected for the [Fe II] abundance determined per star, such that initially $[C/Fe]_o = [N/Fe]_o = [O/Fe]_o = 0.0$. This correction is to simplify the comparison of the A supergiant abundances to CNO-processed solar abundances (which are described by the smooth line in the plot, the "CNO-line"). All three A supergiants lie near the CNO-line, but they do not lie near the first dredge-up predictions of MM. Instead, the abundances appear closer to the point where complete C exhaustion is indicated (where all C has been converted to N by CN-cycling). From the abundances in Table 5, this clearly has not occurred since C is only slightly depleted from solar; also, the average decrease in the carbon abundance for these three stars, $\langle \epsilon(C) - \epsilon(C)_\odot \rangle = (-1.8 \pm 1.2) \times 10^8$, is near the first dredge-up prediction by MM ($= -1.8 \times 10^8$). If CNO-cycling alone is to account for these abundances, then significant mixing of ON-cycled gas must be invoked to drive up the nitrogen abundances.

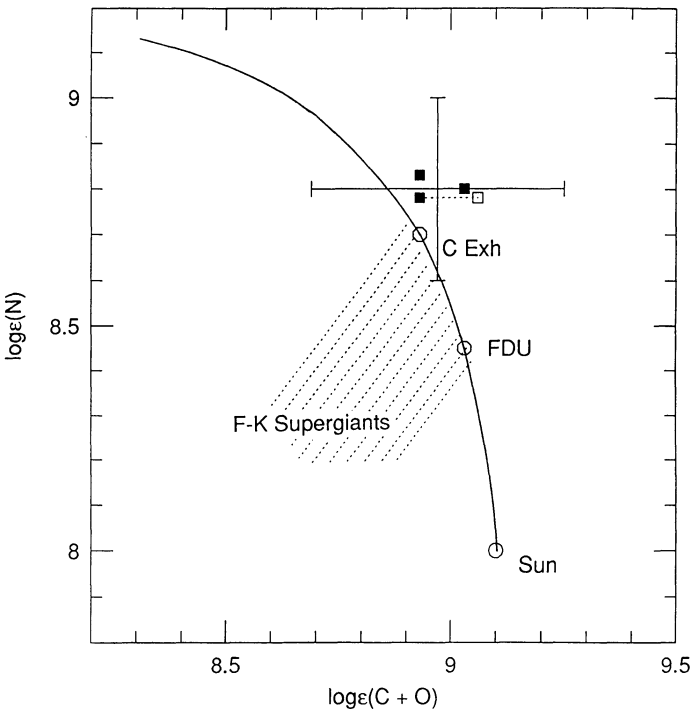

FIG. 8.—Variation in the N abundance with the sum of the C and O abundances for the three A supergiants. The abundances have been corrected for [Fe/H] (see text). For CNO-cycled gas, with an initially solar composition, the abundances would lie along the solid line. The predicted compositions corresponding to first dredge-up (by Maeder & Meynet 1988) and the total conversion of C to N are indicated. Observed abundances for the three A supergiants are marked by solid squares, and the approximate error bar is indicated. The hollow square indicates the abundances for HD 13476 if [O] = 0 (see text). The region of the F-K supergiant abundances is marked (from Luck & Lambert 1985; these abundances have *not* been corrected for [Fe/H]).

Although the O abundances in the A0 Ib stars are near solar, only a small change in log ϵ(O) is required for a significant change in log ϵ(N) [e.g., Δ log ϵ(O) = −0.05 will increase log ϵ(N) by about 0.3 dex]. If significant ON-cycled material is present at the surface, this would require the stellar evolution models to include mixing to deeper interior layers where higher temperatures can drive the ON-cycle efficiently. Also, the evolution scenarios would need to include mixing after the red supergiant phase since significant amounts of ON-cycled gas are not clearly indicated in the F-K supergiant abundances.

Another more likely interpretation is that all of the enhancement of N is not due to CNO-cycling alone. This would be supported by the normal boron abundance reported by Boesgaard & Heacox (1978) in HD 87737 (see § 1.1). Perhaps the nitrogen overabundances indicate a large systematic error in the classical analysis of the N I lines in A supergiant atmospheres. Since the nitrogen abundances are not extremely sensitive to the atmospheric parameters (T, g, ξ; see Table 7), then it is unlikely that the error is in the model atmosphere parameters, particularly since other elements consistently yield near solar or first dredge-up abundances. One possibility is that non-LTE effects are very large in N I line transitions, as calculated by Takeda (1993) for low-metallicity, high-gravity models and by Luck & Lambert (1985) for strong lines. However, only weak lines have been used to calculate the final nitrogen abundances, and Takeda also calculates corrections of only −0.3

dex at solar metallicities (similar to the corrections predicted for the C I and O I line abundances which implies the N/C and N/O ratios would not be significantly affected by departures from LTE). A detailed non-LTE analysis of N I in A supergiants would be very useful in interpreting the nitrogen abundances determined here.

The discussion by Iben & Renzini (1982) of the F-K supergiant abundances shows the importance of also testing the initial abundances assumed. To summarize their discussion; the F-K supergiants were first interpreted as having undergone significant ON-cycling (which is unlike the first dredge-up predictions) because of a N enrichment and significant O depletion (Luck & Lambert 1981). However, Iben & Renzini found (C+O) did not scale with N when initial solar abundances were assumed. By assuming the oxygen abundance had not changed despite the low values derived, they determined that $\langle \epsilon(\mathrm{N}) - \epsilon(\mathrm{N})_\odot \rangle \sim -\langle \epsilon(\mathrm{C}) - \epsilon(\mathrm{C})_\odot \rangle$, and in reasonable agreement with the first dredge-up predictions. A follow-up study of more stars by Luck & Lambert (1985) concluded that primordial O was most likely sub-solar; this is also supported by less than solar O abundances found in main sequence B stars (Gies & Lambert 1992 and references therein). As a test of the initial abundances, we have examined the CNO abundances determined for the B stars by Gies & Lambert (1992). They found $\log \epsilon(\mathrm{C}) = 8.20$, $\log \epsilon(\mathrm{N}) = 7.81$, $\log \epsilon(\mathrm{O}) = 8.68$, and $\log \epsilon(\mathrm{Fe}) = 7.72$. If these abundances are adopted, then the sum $[(\mathrm{C+N+O})/\mathrm{Fe}] \sim +0.6$ for all three A supergiants, and these stars are overabundant in C, N, and O (with the exception of HD 46300 for which C is unchanged, although [C/Fe] is enhanced). This result could be meaningful if not only CNO-cycled gas was mixed to the surface, but also material that has been processed by helium burning. However, this would require the A supergiants to be much more evolved and mixed than is currently predicted, especially when compared to the near first dredge-up abundances determined for the similar mass, F-K supergiants. As another test of the initial abundances, we also examined the mean B-star CNO abundances in h and χ Per determined by Dufton et al. (1990), since HD 13476 is an outlying member of Per OB1. Dufton et al. found $\langle \log \epsilon(\mathrm{C}) \rangle = 7.8 \pm 0.2$, $\langle \log \epsilon(\mathrm{N}) \rangle = 7.8 \pm 0.3$, $\langle \log \epsilon(\mathrm{O}) \rangle = 8.9 \pm 0.3$, and Mg and Si are near solar. If these mean abundances were the initial CNO abundances for HD 13476 then this would require both C and N to now be enhanced, yet O to be depleted, which would be a very puzzling abundance pattern.

For HD 13476, we also note that the [C/O] ratio is larger than predicted by 0.2 dex relative to the MM models. This is due to the odd result that [C/Fe] > [O/Fe] by 0.1 dex. These abundance results are most likely due to uncertainties in the analysis, although the low O abundance is reminiscent of the low O abundances determined for the F-K supergiants by Luck & Lambert (1985) and the B stars by Gies & Lambert (1992 and references therein). If O is unchanged from its initial abundance (thus no ON-cycling), then this point can be plotted in Figure 8 by letting $(\mathrm{C+O}) = (\mathrm{C+O}_\odot)$, which moves this star away from the CNO-line and supports the suggestion that high N abundances are not due to CN-cycling alone.

A larger sample of stars is needed to examine the generality of the CNO abundances in the three A supergiants presented here, and to test for systematic errors in the abundances, particularly N, with temperature and gravity. A detailed non-LTE analysis of N I in A supergiants is also required to test the importance of this effect on the LTE abundances calculated for these stars. Ultimately, we would like to be able to compare the CNO abundances derived for A supergiants to those for B-type and F-K supergiants to study massive star evolution across the HR diagram. Finally, knowing the abundance results for normal A supergiants will also be important for studying other populations of these stars such as the Population II, the high Galactic latitude, and the alleged anomalous A supergiants.

I would like to thank Chris Sneden for his support and involvement in this project, and Michael Lemke for his generous help in operating the ATLAS9, WIDTH, and BALMER codes. Many thanks to David Lambert, Doug Gies, Craig Wheeler, Ed Fitzpatrick, and Harriet Dinerstein, for the helpful discussions and their careful readings of this manuscript. Thanks also to the McDonald Observatory staff for their assistance in operating the telescopes and instruments. I would like to acknowledge making use of the SIMBAD data base, operated by CDS, Strasbourg, France.

REFERENCES

Allen, C. W. 1973, Astrophysical Quantities (London: Athlone Press)
Anders, E., & Grevesse, N. 1989, Geochim. Cosmochim. Acta, 53, 197
Aydin, C. 1972, A&A, 19, 359
Baschek, B., Scholz, M., & Sedlmayr, E. 1977, A&A, 55, 375
Becker, S. A., & Iben, I., Jr. 1979, ApJ, 232, 831
Blackwell, D. E., Petford, A. D., & Simmons, G. J. 1982, MNRAS, 201, 595
Blazit, A., Bonneau, D., Koechlin, L., & Labeyrie, A. 1977, ApJ, 214, L79
Boesgaard, A. M., & Heacox, W. D. 1978, ApJ, 226, 888
Böhm-Vitense, E. 1979, ApJ, 234, 521
Bond, H. E., & Luck, R. E. 1987, ApJ, 312, 203
Boyarchuk, A. A., Lyubimkov, L. S., & Sakhibullin, N. A. 1985, Astrophysics, 22, 203
Crawford, D. L. 1974, AJ, 79, 687
Dufton, P. L., Brown, P. J. F., Fitzsimmons, A., & Lennon, D. L. 1990, A&A, 232, 431
Fitzgerald, M. P. 1970, A&A, 4, 234
Fitzpatrick, E. L., & Garmany, C. D. 1991, ApJ, 363, 119
Frandsen, S. 1974, A&A, 37, 139
Fuhr, J. R., Martin, G. A., & Wiese, W. L. 1988, J. Phys. Chem. Ref. Data, 17, Suppl. No. 4
Fuhr, J. R., Martin, G. A., Wiese, W. L., & Younger, S. M. 1981, J. Phys. Chem. Ref. Data, 10, 305
Gies, D. R., & Lambert, D. L. 1992, ApJ, 387, 673
Gigas, D. 1986, A&A, 165, 170
———. 1988, A&A, 192, 264
Gray, R. O. 1992, A&A, 265, 704
Grevesse, N., Lambert, D. L., Sauval, A. J., van Dishoeck, E. F., Farmer, C. B., & Norton, R. H. 1990, A&A, 232, 225
———. 1991, A&A, 242, 488
Groth, H. 1961, Z. Ap., 51, 206
Hibbert, A., Biémont, E., Godefroid, M., & Vaeck, N. 1992, A&A, preprint
———. 1991a, J. Phys B: At. Mol. Opt. Phys., 24, 3943
———. 1991b, A&AS, 88, 505
Hill, G. M., Walker, G. A. H., & Yang, S. 1986, PASP, 98, 1186
Humphreys, R. M., Kudritzki, R. P., & Groth, H. 1991, A&A, 245, 593
Hutchings, J. B. 1976, Publ. Dom. Ap. Obs., 14, 355
Iben, I. Jr., & Renzini, A. 1982, ARA&A, 21, 271
Ivanova, Z. K., & Lyubimkov, L. S. 1990, Bull. Crimean Astrophys. Obs., 79, 45
Konjevic, N., & Roberts, J. R. 1976, J. Phys. Chem. Ref. Data, 5, 209
Kudritzki, R. P. 1973, A&A, 28, 103
Kurucz, R. L. 1979, ApJS, 40, 1
———. 1990, Trans. Int. Astron. Union, B20, 168: magnetic tape
Lambert, D. L., Hinkle, K. H., & Luck, R. E. 1989, ApJ, 333, 917
Lambert, D. L., Roby, S. W., & Bell, R. A. 1982, ApJ, 254, 663
Lester, J. B., Gray, R. O., & Kurucz, R. L. 1986, ApJS, 61, 509
Lobel, A., Achmad, L., de Jager, C., & Nieuwenhuijzen, H. 1992, A&A, 256, 159
Luck, R. E., & Bond, H. E. 1984, ApJ, 279, 729
Luck, R. E., Bond, H. E., & Lambert, D. L. 1990, ApJ, 357, 188
Luck, R. E., & Lambert, D. L. 1981, ApJ, 245, 1018
———. 1985, ApJ, 298, 782

Lyubimkov, L. S., & Boyarchuk, A. A. 1983, Astrophysics, 19, 385
Maeder, A., & Meynet, G. 1988, A&AS, 76, 411 (MM)
Martin, G. A., Fuhr, J. R., & Wiese, W. L. 1988, J. Phys. Chem. Ref. Data, 17, Suppl. No. 3
Moon, T. T., & Dworetsky, M. M. 1985, MNRAS, 217, 305
Moore, C. E. 1952, NSRDS-NBS, Circ. 467
———. 1970, NSRDS-NBS, 3
———. 1972, NSRDS-NBS, 40
Nussbaumer, H., & Storey, P. J. 1984, A&A, 140, 383
O'Brian, T. R., Wickliffe, M. E., Lawler, J. E., Whaling, W., & Brault, J. W. 1991, Opt. Soc. Am., B8, 1185
Parsons, S. B. 1967, ApJ, 150, 263
Percy, J. R., & Welch, D. L. 1983, PASP, 95, 491
Przybylski, A. 1969, MNRAS, 146, 71
Relyea, L. J., & Kurucz, R. L. 1978, ApJS, 37, 45
Rosendhal, J. D. 1970, ApJ, 160, 627
Russell, S. C., & Bessell, M. S. 1989, ApJS, 70, 865
Schaller, G., Schaerer, D., Meynet, G., & Maeder, A. 1992, A&AS, 96, 269
Sigut, T. A. A., & Landstreet, J. D. 1990, MNRAS, 247, 611
Strömgren, B., Olsen, E. H., & Gustafsson, B. 1982, PASP, 94, 5
Stürenberg, S., & Holweger, H. 1990, A&A, 237, 125
Takeda, Y. 1993, PASJ, in press
van Genderen, A. M. 1989, A&A, 208, 135
Vidal, C. R., Cooper, J., & Smith, E. W. 1973, ApJS, 25, 37
Wiese, W. L., & Martin, G. A. 1980, NSRDS-NBS, 68
Wiese, W. L., Smith, M. W., & Miles, B. M. 1969, NSRDS-NBS, 22
Wolf, B. 1971, A&A, 10, 383
Zhu, Q., Bridges, J. M., Hahn, T., & Wiese, W. L. 1989, Phys. Rev. A, 40, 3721